

1 **The Open Perimetry Initiative: a framework for cross-platform development for the new generation of portable**  
2 **perimeters**

3 Iván Marín-Franch<sup>1</sup>, Andrew Turpin,<sup>2</sup> Paul H Artes<sup>3,4</sup>, Luke X Chong<sup>5</sup>, Allison M McKendrick<sup>6</sup>, Karam A Alawa<sup>7</sup>,  
4 Michael Wall<sup>7</sup>

5 <sup>1</sup> Computational Optometry, Atarfe, Spain

6 <sup>2</sup> School of Computing and Information Systems, University of Melbourne, Melbourne, Victoria, Australia

7 <sup>3</sup> Southwest Eye Institute, Tavistock, UK

8 <sup>4</sup> Eye & Vision Research Group, School of Health Professions, University of Plymouth, Plymouth, UK

9 <sup>5</sup> School of Medicine (Optometry), Deakin University, Geelong, Australia

10 <sup>6</sup> Department of Optometry and Vision Sciences, University of Melbourne, Melbourne, Victoria, Australia

11 <sup>7</sup> Departments of Neurology and Ophthalmology and Visual Sciences, University of Iowa, College of Medicine, Iowa  
12 City, Iowa, USA

13 **Corresponding author:**

14 Iván Marín-Franch, PhD

15 Computational Optometry, Atarfe, Spain

16 Phone no: +34 609 612 780.

17 Email: [imarinfr@optocom.es](mailto:imarinfr@optocom.es)

18 **Funding:** Veterans Administration Merit Review (I01 RX-001821-01A1)

19 **Abstract**

20 The Open Perimetry Initiative is fully open source and consists of the Open Perimetry Interface (OPI) and an  
21 accompanying package (visualFields) with analytical tools. The OPI package contains an ever-growing number of  
22 drivers for commercially available perimeters, head-mounted devices, and virtual reality headsets. The visualFields  
23 package contains tools for the analysis and visualization of visual field data, including methods to compute  
24 deviation values and probability maps. The use of the OPI and visualFields is shown through a custom static  
25 automated perimetry test for the full visual field (up to 50° nasally and 80° temporally) developed with the OPI  
26 driver for the Octopus 900 and using visualFields for statistical analysis. Its potential for the development of cross-  
27 platform apps for driving and testing portable devices is demonstrated with an OPI driver for an Android-based  
28 headset. With more than 55 citations in clinical and translational science as listed in Scopus, this initiative has  
29 contributed significantly to expanding the knowledge base in perimetry and clinical vision research at large, and  
30 with clinical translation. The continued support of researchers, clinicians, industry, and public institutions are key  
31 in transforming perimetry research from closed to open science. The Open Perimetry Initiative provides framework  
32 to achieve this.

### 33 **Introduction**

34 The advent of new technologies and the development of cross-platform software are paving the way for a new  
35 wave of portable devices for visual field testing. The transition from traditional projection perimetry to display-  
36 based perimetry requires analysis and adaption of conventional perimetry methods and provides an opportunity  
37 to revise and improve.

38 The Open Perimetry Initiative is an open-source project that started in 2010 with the goal of alleviating the  
39 difficulties of using commercial and experimental ophthalmic devices in vision research. The initiative has evolved  
40 beyond its original goal to also include features that facilitate the development of new paradigms, standards, and  
41 good practices that exploit the technological advantages of portable devices. To maximize accessibility of novel  
42 perimetry methods and techniques, implementations using the Open Perimetry libraries are expected to be open  
43 source under the GNU General Public License. To avoid the possible legal ramifications, permission from device  
44 manufacturers is required before OPI code is used on their commercial instruments.<sup>1</sup>

45 The key product of the Open Perimetry Initiative is the Open Perimetry Interface (OPI).<sup>1</sup> The OPI not only provides  
46 drivers for an increasing number of ophthalmic devices, but it also sets standards and protocols for the  
47 implementation of custom visual field tests so that they can be run seamlessly on different machines, with one  
48 implementation for many devices. Furthermore, the OPI can be run in simulation mode, so that new perimetric  
49 procedures can be implemented, debugged, and assessed before they are ported to the actual test device. The  
50 second key product of the Open Perimetry Initiative is visualFields.<sup>2</sup> This R package<sup>3</sup> is a tool for the statistical  
51 analysis and visualization of perimetry results. Until now, the OPI and visualFields solutions have been developed  
52 largely independently from one another. Recent developments in R, in particular the shiny package<sup>4</sup>  
53 (<https://shiny.rstudio.com>), have made it possible to easily develop cross-platform applications with graphical  
54 interfaces that integrate the OPI and visualFields software.

55 The purpose of this paper is to describe the recent advances in both the OPI and visualFields and to showcase their  
56 use in conventional perimeters as well as new devices such as tablets, phones, and virtual reality headsets. In  
57 addition to the development of novel paradigms, methods, and software, the optical properties need to be  
58 characterized on these new devices, including resolution and the effects of chromatic and achromatic aberrations.  
59 It is likewise necessary to develop adequate methods for calibration and compensation of refractive errors.  
60 Considerations of optical characterization, calibration, and limitations are beyond the scope of this manuscript.

## 61 **Methods**

62 The OPI has drivers for the Octopus 900 perimeter (Haag-Streit AG, Köniz, Switzerland), the Compass  
63 microperimeter (Centervue, Padova, Italy), and the AP-7000 perimeter (Kowa, Torrance, CA, USA). New drivers  
64 have now been incorporated for the IMO (CREWT Medical Systems, Tokyo, Japan) and for the Google Cardboard,  
65 Google Daydream, and other Android-compatible head-mounted displays. Drivers for devices such as the VIVE Pro  
66 Eye (HTC Corporation, Taoyuan City, Taiwan) and AVA Advanced Vision Analyzer (Elisar, India) are being developed.

### 67 OPI conventions and standards

68 The OPI implementations and drivers follow conventions and standards that not only accelerate software  
69 development, but also enable the creation of custom tests, perimetric algorithms, and procedures. These can all  
70 be used with different computer operating systems, programming languages, and with different commercial and  
71 experimental perimeters. The OPI commands are described more fully elsewhere<sup>1</sup> but are listed here for  
72 completeness:

- 73 • `opiInitialize()`: open connection with the perimeter and ready it,
- 74 • `opiQueryDevice()`: get information about the perimeter,
- 75 • `opiSetBackground()`: set the background color, luminance, fixation point, etc.,
- 76 • `opiPresent()`: Present a stimulus and return observer's response, and
- 77 • `opiClose()`: close the connection with the perimeters

78 There are three distinct types of visual field stimuli that can be presented with the `opiPresent()` command: static,  
79 temporal, and kinetic. The static type can be used for conventional static automated perimetry.<sup>5,17,18</sup> The temporal  
80 type can be used to generate stimuli that vary over time and that are supported by the underlying hardware, such  
81 as the frequency-doubling illusion<sup>19,20</sup>. The kinetic type can be used to present moving stimuli specified according  
82 to the nomenclature introduced by Hans Goldmann.<sup>21</sup> The `opiPresent()` command returns the response of the  
83 observer (whether the response button was pressed or not after a stimulus presentation and the time between  
84 onset of stimulus presentation and response), and the pupil position at the time the button was pressed (if  
85 hardware allows).

86 It is possible to interact with the perimeter via the `opiPresent()` command and build a stimulus-response logic from  
87 which complex test procedures can be constructed. Several common procedures are already built into the OPI  
88 package:

- 89 • `MOCS()`: The method of constant stimulus or MOCS,<sup>22</sup>
- 90 • `fourTwo()`: The 4-2 dB staircase,<sup>23,24</sup>
- 91 • `FT()`: The full threshold algorithm,<sup>23,24</sup> and
- 92 • `ZEST()`: The Bayesian QUEST and ZEST algorithms<sup>25</sup>

93 The implementation of the aforementioned OPI commands and drivers are necessarily different for each different  
94 perimeter; however, the specific implementation can be selected with the command `opiChoose()`. Thus, once a  
95 specific perimetry driver —Octopus900, Compass, IMO, Daydream, etc.— has been selected, a dispatcher is set in place  
96 so that the same OPI commands listed earlier can be used without change with all supported hardware.

97 Using the same approach, it is possible to generate graphical user interfaces that are platform-independent (e.g.,  
98 the R package `shiny`<sup>4</sup>), which provides a framework for developing interactive web apps. Shiny was used to develop  
99 applications to drive the Octopus 900 perimeter and the Google Daydream headset (shown in Results in this  
100 manuscript). The Daydream shiny app allows one to configure the device and perimetry test, obtain the luminance

101 profile (i.e., the correspondence between pixel value and physical luminance, of compatible Android phones),  
102 manage datasets, run a threshold test on conventional and custom grids of test locations, and generate graphical  
103 reports from the results.

#### 104 The visualFields analytical tool

105 The visualFields package has undergone a major revision moving from version 0.6<sup>2</sup> to version 1.0 introduced here. Its  
106 core functionality is the same but the code has been simplified; some dated ideas and methods have been  
107 deprecated, and a number of conventions have been adopted for clarity and simplicity. The most visually striking  
108 change has been the adoption of Voronoi tessellation<sup>26–28</sup> for the graphical representation of visual field data and  
109 statistics. In addition, an effort has been made to improve its transparency and the reproducibility of its methods.  
110 For instance, the SUNY-IU dataset of healthy subjects that was used in the previous version to generate normative  
111 values has been incorporated into the package, `vfctrSunyiu24d2`, along with a function that generates the normative  
112 reference values. Thus, the command `nvgenerate(vfctrSunyiu24d2)` generates pointwise normative values and the  
113 command `nvgenerate(vfctrSunyiu24d2, method = "smooth")` generates the normative values used in the visualFields 0.6<sup>2</sup> using  
114 the smoothing techniques as those introduced by Heijl and colleagues for the Statpac 2.<sup>29,30</sup> Normative datasets,  
115 `vfctrIowaPC26` and `vfctrIowaPeri`, and reference values generated with the function `nvgenerate` for the custom tests used  
116 to study the advantages of exploring the full visual field are also included in the package.<sup>8–11</sup>

#### 117 Data availability

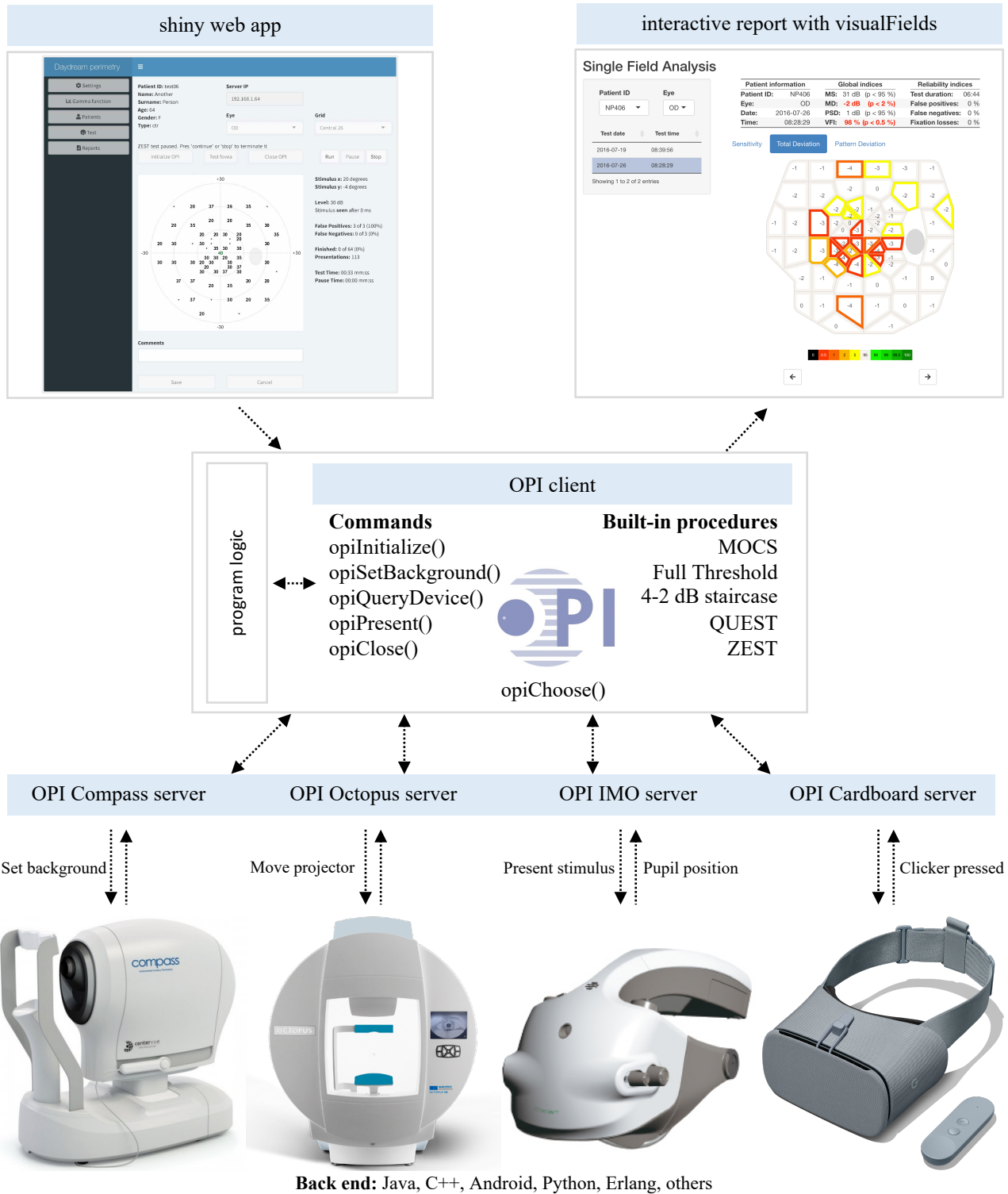
118 The release version of OPI can be found at <https://CRAN.R-project.org/package=OPI>. The release version of  
119 visualFields can be found at <https://CRAN.R-project.org/package=visualFields>. The development version of OPI can  
120 be found at <https://github.com/turpinandrew/OPI>. The development version of visualFields can be found at  
121 <https://github.com/imarinfr/vf1>. Most datasets used in this manuscript can be found within the visualFields  
122 package. The dataset of healthy subjects for the full visual field can be found in the visualFields package as well as  
123 in <https://www.sciencedirect.com/science/article/pii/S2352340918311570>. The applications developed based on

124 the OPI and visualFields packages and presented in the manuscript, as well as the datasets are available from the  
125 corresponding author on reasonable request.

## 126 **Results**

127 **Figure 1** illustrates the OPI architecture. Once the hardware is selected, the R OPI client dispatches the commands  
128 to connect, disconnect, set background and other settings, and present stimuli to the corresponding OPI server  
129 (Octopus 900, Compass, IMO, Cardboard, etc.), which ultimately communicates the commands to the hardware.  
130 The server then waits for the hardware to send its state or respond (machine initialized, background lit, pupil  
131 position, clicker pressed within a time response window after stimulus onset, etc.) and communicates the response  
132 to the OPI client. A web app, as the one shown in the top left of **Figure 1** in R with the shiny package, can be  
133 developed on top of a program logic to run conventional or custom visual field tests on both regular or irregular  
134 grids of test locations with the OPI built-in algorithms (ZEST, full threshold, etc.). It also has the capability to run  
135 other procedures, including a suprathreshold test due to Aulhorn<sup>5</sup> or the binocular Esterman test.<sup>6</sup> Port  
136 communication via internet protocol networks and listeners in the program logic allows for separation of the front-  
137 end and the OPI client back-end. This way, the web app used as front-end is easily replaceable by any other front-  
138 end developed in Java, Python, MATLAB, or any other suitable programming language. Port communication in R  
139 was achieved by creating a background R session with the callr package<sup>7</sup> that runs in parallel. With this architecture,  
140 the program logic embedding the OPI client runs in the background while the web app runs in parallel in the  
141 foreground.

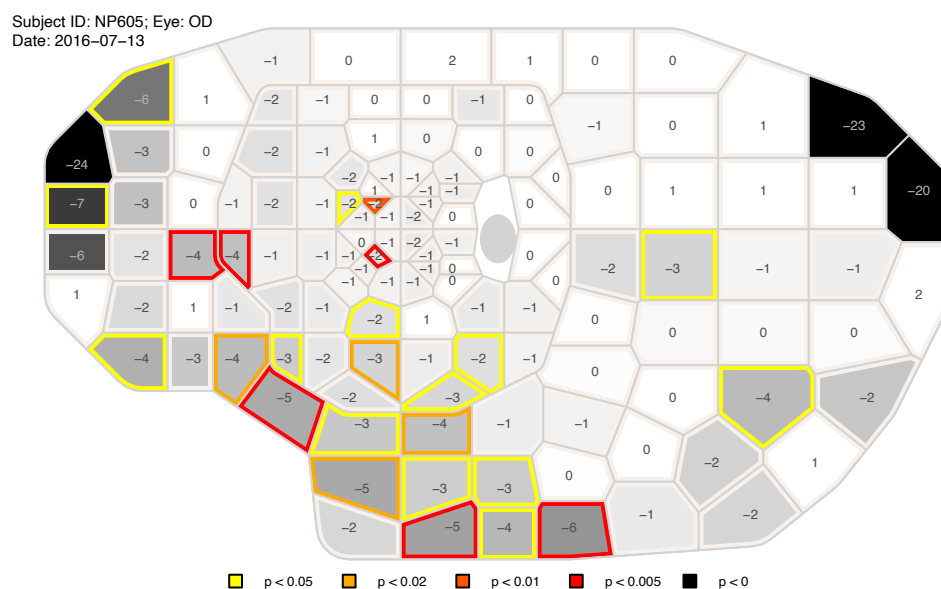
Front end: R, Python, MatLab, Java, HTML, others



142 **Figure 1: Illustration of the OPI architecture.** Top left is a graphical interface generated in shiny for a program logic that can be run on any  
 143 device at the bottom through the OPI client (center) as it dispatches commands via the OPI servers. Once a suitable dataset of healthy controls  
 144 has been collected, statistical analyses as the one in the top right can be generated with the visualFields package.



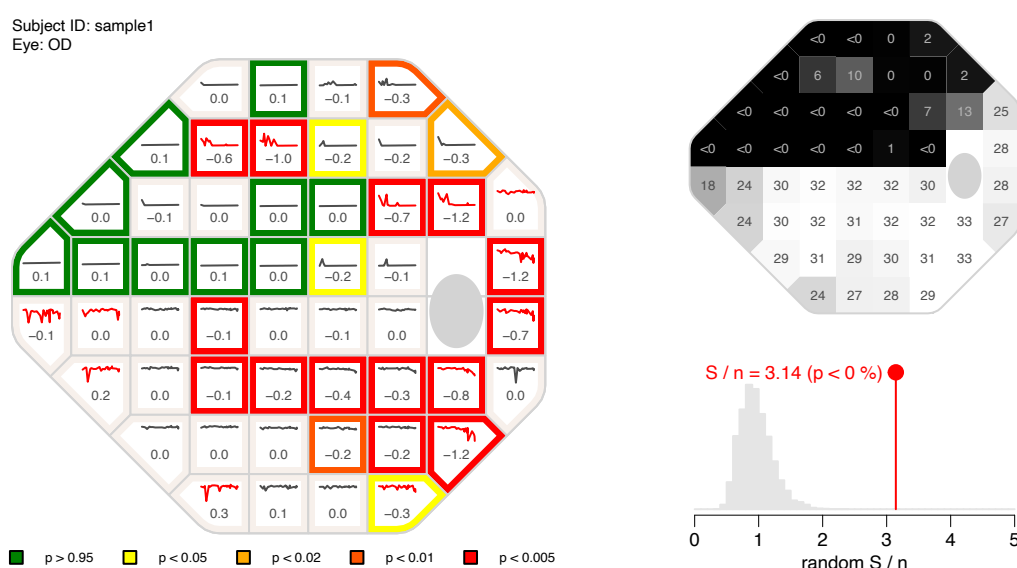
145 The OPI was used to run a series of tests of the full visual field.<sup>8-11</sup> A publicly available dataset of 98 eyes of 98  
146 healthy subjects<sup>8</sup> was used to derive normative values with the visualFields R package.<sup>2</sup> Figure 2 shows a statistical  
147 analysis of the results for a specific full visual field, which consists of the combined analysis of two tests taken on  
148 the same day, one for the central visual field and another for the far periphery.<sup>8-11</sup> The tiles involving each visual  
149 field location were obtained using Voronoi tessellation to achieve an efficient representation for both highly  
150 irregular grids. Voronoi tessellations are a partitioning of a surface into regions so that the center of each cell is its  
151 mean (center of mass). Every point in a given Voronoi polygon is closer to its generating point than to any other  
152 cell. We believe this type of graphic best represents the visual area tested, without interpolating between different  
153 points. The dataset of ocular healthy eyes<sup>8</sup> is incorporated in the visualFields 1.0 for the central and peripheral tests,  
154 `vfctrlowaPC26` and `vfctrlowaPeri`. A script that generates figures for all subjects in those datasets is provided as  
155 supplemental material with name `vfPlotFullField.r`.



156 **Figure 2: Combined grayscale sensitivity and color-coded total-deviation map.** The representation of the full visual field results are  
157 composites of two tests taken on the same day: one spanning the central 26° of the visual field and another from 26° to 50° nasally, to 80°  
158 temporally, to 50° inferiorly, and to 46° superiorly. The values shown at each location are total deviations, departures in sensitivity from the  
159 mean normal sensitivities for age-matched controls. The background grayscale of each tile represents the estimated sensitivity at the  
160 corresponding visual field location, where darker means lower sensitivity. Tiles whose border is shown in color are significantly depressed  
161 according to the statistical analysis of the total-deviation map. Locations with total-deviation values below the percentile 0.5 from age-  
162 corrected mean normal are red, those below the percentile 1 are dark orange, those below the percentile 2 are light orange, and those below  
163 the percentile 5 are yellow.

164

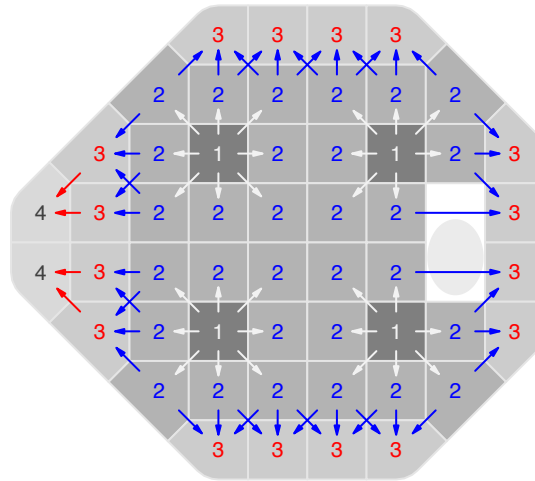
165 In addition to these single field analyses, the visualFields package also has tools to analyze longitudinal data,  
 166 including pointwise linear regression, and the permutation of pointwise linear regression, or PoPLR.<sup>12</sup> Figure 3  
 167 shows a brief report (generated with the script vfPoPLRAnalysis.r provided as supplemental material and with the  
 168 vfpwgSunyiu24d2 dataset<sup>13</sup>). The normative values to obtain total deviation values and probability maps were  
 169 generated using the dataset, vfctrSunyiu24d2, from a prospective longitudinal study conducted Bloomington, Indiana  
 170 University (IU) and New York City, State University of New York (SUNY).<sup>2</sup> The normative values were obtained with  
 171 the command nvgenerate(vfctrSunyiu24d2).



172 **Figure 3: The PoPLR analysis.** The left panel shows the slopes at each visual field location obtained with pointwise linear regression of total  
 173 deviation values over time along with sparklines representing the values over the whole series. The colors at the border of the tiles represent  
 174 different  $p$ -values, with red representing a  $p$ -value lower than 0.5% for the 1-tail  $t$ -test with the alternative that the slope is negative, dark  
 175 orange representing  $p$ -values lower than 1%, light orange representing  $p$ -values lower than 2%, yellow representing  $p$ -values lower than 5%,  
 176 and green representing  $p$ -values greater than 95%. To identify highly variable series of visual fields, the sparklines are shown in red if the  
 177 median absolute deviation of the residuals from linear regression were greater than 2 dB. The top right function shows a grayscale map of the  
 178 baseline sensitivity values (intercept of pointwise regression on sensitivities). The bottom right function shows the histogram of random  $S/n$ ,  
 179 where  $n$  is the number (52 in this case) of regression analyses performed obtained by permuting the series as part of the PoPLR analysis. The  
 180  $p$ -value for the PoPLR analysis testing whether there is deterioration is shown next to the value of the observed  $S/n$  statistic.

181  
 182 The ZEST algorithm parametrization used to measure the full visual field<sup>8-11</sup> has been updated and improved for its  
 183 use with an experimental Daydream OPI perimeter. The specific implementation of the ZEST algorithm has a  
 184 bimodal prior probability mass function with one peak centered at 0 dB to model sensitivities of damaged locations  
 185 and another peak that depends on sensitivity estimates in neighboring locations.<sup>14</sup> Neighboring locations are now

186 defined as locations that share line segments which formed the polygons obtained via Voronoi tessellation. [Figure](#)  
187 [4](#) shows the Voronoi tessellation pattern for the 24-2 grid of test locations, with arrows indicating how locations  
188 are sampled following a growth algorithm. A conventional 24-2 grid was used instead of the irregular one in [Figure](#)  
189 [2](#) for clarity of illustration.

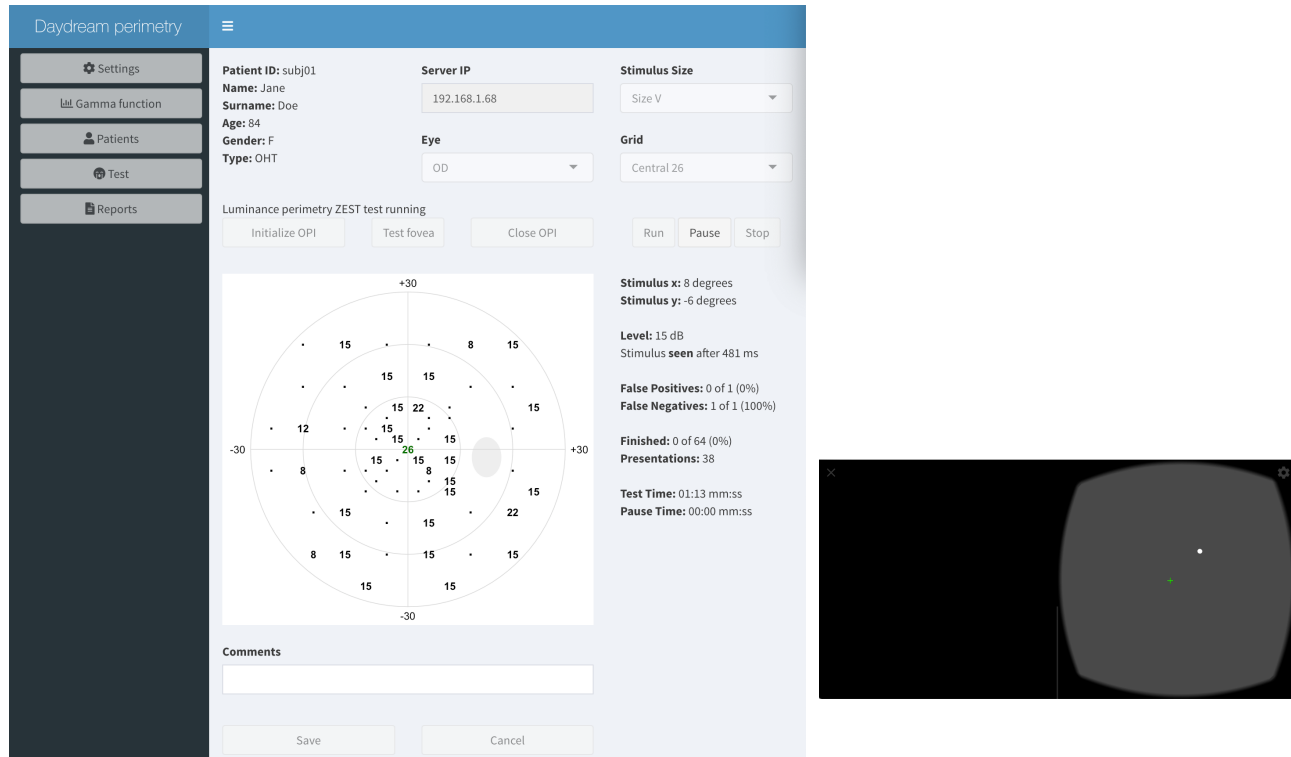


190 **Figure 4: The growth algorithm.** The numerals represent the growth pattern wave number of the 52 locations (after excluding the two closest  
191 to the blind spot) of the 24-2 regular grid of test locations. Locations corresponding to the primary wave are labelled with the number 1, and  
192 locations corresponding to the second, third, and fourth waves are respectively labelled with the numbers 2, 3, and 4. The polygons that  
193 determine each location's wave and neighbors were obtained using Voronoi tessellation and are shown in 4 shades of gray, from dark to light,  
194 corresponding to the 4 waves of the growth algorithm.

195

196 The growth pattern applied to the 24-2 grid consists of 4 waves and commences at four primary locations (labelled  
197 as "1" in [Figure 3](#)). At the beginning, only these four primary locations are tested at random, with the second peak  
198 of the bimodal probability mass function at 30 dB. Once a primary location is complete, its neighboring locations  
199 that correspond to the second wave (labelled as "2" in [Figure 3](#)) open up for testing, with the second peak centered  
200 at the posterior estimated sensitivity threshold of its predecessor. Once a location of the second wave is complete,  
201 it propagates its estimated sensitivity threshold to its neighbors that correspond to the third wave (labelled as "2"  
202 in [Figure 3](#)) and so on and until all locations have been completed. The growth algorithm should not propagate

203 through the midline since the ganglion cells on the upper and lower hemifields follow different trajectories<sup>15</sup> and  
204 therefore there is no structural correlation between those neighboring visual field locations.



205 **Figure 5: Shiny web app for the OPI Daydream server.** The ZEST algorithm for luminance (white-on-white) perimetry for a custom  
206 irregular grid of test locations is executed for a (fictitious) patient with ocular hypertension using a web app developed in shiny (left panel).  
207 The web app sends commands to an Android Pixel 3 phone (shown in the right panel) to generate white visual stimuli at different intensities  
208 and at different distances from the fixation point (green cross). At each presentation, the web app updates and shows the interim results of the  
209 test. This screenshot was possible thanks to screpy (<https://github.com/Genymobile/screpy>).

210

211 **Figure 5** shows a web app developed for the Daydream OPI running the updated ZEST algorithm with an irregular  
212 grid of test locations, that corresponds to the central part in the full visual field tests.<sup>8-11</sup> Although in this application  
213 the background was black for the contralateral eye (left half of the screen), the Daydream OPI implementation  
214 allows for the presentation of the same background luminance on both eyes.

## 215 Discussion

216 The advent of new technologies and the development of cross-platform software are preparing the way for a new  
217 wave of portable devices for visual field testing. To lay the groundwork for this new era of perimetry, it is important

218 to build a knowledge base on the strengths and weaknesses of the coming generation of perimeters, as well as  
219 revise and accommodate conventional methods and analyses to unveil their full potential. It is essential to do this  
220 in a manner that is as transparent and as accessible as possible by adhering to the open science principles (open  
221 source, open data, and open access).<sup>16</sup>

222 The Open Perimetry Initiative and other open-source initiatives that expand perimetry knowledge base and make  
223 it freely accessible are essential to equip clinicians and researchers with the necessary tools to objectively assess  
224 different products and solutions for the coming generation of portable perimeters. Furthermore, its drivers,  
225 applications, and carefully curated datasets collected as a result of these open-source initiatives are beneficial for  
226 research groups and institutions, not-for-profit organizations, private entrepreneurs, and eye care at large. The  
227 Open Perimetry Initiative continues to have a beneficial impact on perimetry and vision research. As of May 2021,  
228 OPI and visualFields related publications received 57 peer-reviewed citations from 12 countries in 4 continents (see  
229 [Figure 6](#), data from Scopus). received a total of Its popularity is growing as the yearly average number of citations  
230 went from 5.3 before 2018 to 8.3.



231 **Figure 6: Geographical map of citations to the OPI and the visualFields R package as listed in the ISI Web of Science.** The red solid  
232 circles demarcate the cities of the first authors' affiliations. The sizes of the circles represent the number of citations from each city, up to  
233 three.

234 The Open Perimetry Initiative would not have evolved had it not been for the generosity and active support of key  
235 researchers, clinicians, industry, and public institutions. It now needs the involvement of new researchers,  
236 clinicians, and entrepreneurs to continue its development.

### 237 **Acknowledgements**

238 Veterans Administration Merit Review (I01RX-001821-01A1) and This work was supported by Computational  
239 Optometry (Atarfe, Spain, URL: [www.optocom.es](http://www.optocom.es)). We thank Jize Dong for writing the initial versions of the Java  
240 code for the OPI Daydream/Cardboard server. We also thank Zachary Heinzman for reviewing the manuscript.

### 241 **References**

- 242 1. Turpin, A., Artes, P. H. & McKendrick, A. M. The Open Perimetry Interface: an enabling tool for clinical  
243 visual psychophysics. *J. Vis.* **12**, 22 (2012).
- 244 2. Marín-Franch, I. & Swanson, W. H. The visualFields package: A tool for analysis and visualization of visual  
245 fields. *J. Vis.* **13**, 1-12,10 (2013).
- 246 3. R Core Team. R: A Language and Environment for Statistical Computing. (2021).
- 247 4. Chang, W., Cheng, J., Allaire, J., Xie, Y. & McPherson, J. shiny: Web Application Framework for R. (2020).
- 248 5. Aulhorn, E. & Harms, H. Early visual field defects in glaucoma. in *Glaucoma Tutzing Symposium* (ed.  
249 Leydhecker, W.) (S. Karger, Ltd, 1967).
- 250 6. Esterman, B. Functional Scoring of the Binocular Field. *Ophthalmology* **98**, 1226–1234 (1982).
- 251 7. Csárdi, G. & Chang, W. callr: Call R from R. (2020).
- 252 8. Marín-Franch, I., Artes, P. H., Chong, L. X., Turpin, A. & Wall, M. Data obtained with an open-source static  
253 automated perimetry test of the full visual field in healthy adults. *Data Br.* **21**, 75–82 (2018).
- 254 9. Wall, M. *et al.* Threshold Automated Perimetry of the Full Visual Field in Patients with Glaucoma with Mild  
255 Visual Loss. *J. Glaucoma* **28**, 997–1005 (2019).
- 256 10. Wall, M. *et al.* Threshold static automated perimetry of the full visual field in idiopathic intracranial  
257 hypertension. *Investig. Ophthalmol. Vis. Sci.* **60**, 1898–1905 (2019).

- 258 11. Wall, M., Lee, E. J., Wanzek, R. J., Chong, L. X. & Turpin, A. Temporal Wedge Defects in Glaucoma. *J.*  
259 *Glaucoma* **29**, 191–197 (2020).
- 260 12. O’Leary, N., Chauhan, B. C. & Artes, P. H. Visual field progression in glaucoma: estimating the overall  
261 significance of deterioration with permutation analyses of pointwise linear regression (PoPLR). *Investig.*  
262 *Ophthalmol. Vis. Sci.* **53**, 6776–6784 (2012).
- 263 13. Artes, P. H., O’Leary, N., Nicolela, M. T., Chauhan, B. C. & Crabb, D. P. Visual Field Progression in  
264 Glaucoma: What Is the Specificity of the Guided Progression Analysis? *Am. Acad. Ophthalmol.* **121**, 2023–  
265 2027 (2014).
- 266 14. Vingrys A. J. Pianta, M. J. Developing a clinical probability density function for automated perimetry. *Aust.*  
267 *N. Z. J. Ophthalmol.* **26**, S101–S103 (1998).
- 268 15. Jansonius, N. M. *et al.* A mathematical description of nerve fiber bundle trajectories and their variability in  
269 the human retina. *Vision Res.* **49**, 2157–2163 (2009).
- 270 16. Vicente-Saez, R. & Martinez-Fuentes, C. Open Science now: A systematic literature review for an  
271 integrated definition. *J. Bus. Res.* **88**, 428–436 (2018).
- 272 17. Fankhauser, F., Koch, P. & Roulier, A. On Automation of Perimetry. *Albr. Von Graefes Arch Klin Exp*  
273 *Ophthalmol* **184**, 126–150 (1972).
- 274 18. Koch, P., Roulier, A. & Fankhauser, F. Perimetry - the Information Theoretical Basis for its Automation.  
275 *Vision Res.* **12**, 1619–1630 (1972).
- 276 19. Kelly, D. H. Frequency Doubling in Visual Responses. *J. Opt. Soc. Am.* **56**, 1628–1633 (1966).
- 277 20. Maddess, T. & Henry, G. H. Performance of nonlinear visual units in ocular hypertension and glaucoma.  
278 *Clin. Vis. Sci.* **7**, 371–383 (1992).
- 279 21. Goldmann, H. Fundamentals of exact perimetry. 1945. *Optom. Vis. Sci.* **76**, 599–604 (1999).
- 280 22. Fechner, G. T. *Elements of psychophysics*. (Holt, Rinehart & Winston [Original work published in German"  
281 Fechner, G. T., *Elemente der Psychophysik*, Breitkopf und Härtel, Leipzig, 1860"], 1966).

- 282 23. Bebie, H., Fankhauser, F. & Spahr, J. Static perimetry: strategies. *Acta Ophthalmol.* **54**, 325–338 (1976).
- 283 24. Johnson, C. A., Chauhan, B. C. & Shapiro, L. R. Properties of Staircase Procedures for Estimating Thresholds  
284 in Automated Perimetry. *Investig. Ophthalmol. Vis. Sci.* **33**, 2966–2974 (1992).
- 285 25. King-Smith, P. E., Grigsby, S. S., Vingrys, A. J., Benes, S. C. & Supowit, A. Efficient and Unbiased  
286 Modifications of the QUEST Threshold Method: Theory, Simulations, Experimental Evaluation and Practical  
287 Implementation. *Vision Res.* **34**, 885–912 (1994).
- 288 26. Aurenhammer, F. & Klein, R. Voronoi Diagrams. in *Handbook of computational geometry* (eds. Sack, J. R. &  
289 Urrutia, J.) 201–290 (North-Holland, Elsevier, 1999).
- 290 27. Descartes, R. *Principia Philosophiæ*. (Ludovicus Elzevirius, 1644).
- 291 28. Kucur, Ş. S., Holló, G. & Sznitman, R. A deep learning approach to automatic detection of early glaucoma  
292 from visual fields. *PLoS One* **13**, e0206081 (2018).
- 293 29. Heijl, A., Lindgren, G. & Olsson, J. A package for the statistical analysis of visual fields. *Doc. Ophthalmol.*  
294 *Proc. Ser.* **49**, 153–168 (1987).
- 295 30. Heijl, A. *et al.* Extended empirical statistical package for evaluation of single and multiple fields: Statpac 2.  
296 in *Perimetry Update 1990/1991* (New York: Kugler & Ghedini, 1991).